

# Diffusion models for probabilistic precipitation generation from atmospheric variables

\*

Michael Aich<sup>1,2\*</sup>, Sebastian Bathiany<sup>1,2</sup>, Philipp Hess<sup>1,2</sup>,  
Yu Huang<sup>1,2</sup>, Niklas Boers<sup>1,2,3</sup>

<sup>1</sup>Technical University Munich, Munich, Germany; School of Engineering & Design,  
Earth System Modelling.

<sup>2</sup>Potsdam Institute for Climate Impact Research, Potsdam, Germany.

<sup>3</sup>Global Systems Institute and Department of Mathematics, University of Exeter,  
Exeter, UK.

\*Corresponding author. E-mail: [michael.aich@tum.de](mailto:michael.aich@tum.de);

## Abstract

Improving the representation of precipitation in Earth system models (ESMs) is critical for assessing the impacts of climate change and especially of extreme events like floods and droughts. In existing ESMs, precipitation is not resolved explicitly, but represented by parameterizations. These typically rely on resolving approximated but computationally expensive column-based physics, not accounting for interactions between locations. They struggle to capture fine-scale precipitation processes and introduce significant biases. We present a novel approach, based on generative machine learning, which integrates a conditional diffusion model with a UNet architecture to generate accurate, high-resolution (0.25°) global daily precipitation fields from a small set of prognostic atmospheric variables. Unlike traditional parameterizations, our framework efficiently produces ensemble predictions, capturing uncertainties in precipitation, and does not require fine-tuning by hand. We train our model on the ERA5 reanalysis and present a method that allows us to apply it to arbitrary ESM data, enabling fast generation of probabilistic forecasts and climate scenarios. By leveraging interactions between global prognostic variables, our approach provides an alternative parameterization scheme that mitigates biases present in the ESM precipitation while maintaining consistency with its large-scale (annual) trends. This work demonstrates that complex precipitation patterns can be learned directly from large-scale atmospheric variables, offering a computationally efficient alternative to conventional schemes.

**Teaser:** generative machine learning method replaces column based precipitation parameterization of climate models.

## 1 Introduction

Heavy precipitation events will increase in frequency and magnitude in response to global warming [1, 2]. Extreme precipitation amplifies flood risks and leads to significant infrastructure, economic, and ecological damages [3]. General circulation models (GCMs) are used to simulate precipitation in current and future scenarios to help us understand changes and their impacts on the Earth system and society. Accurate high-resolution precipitation simulations are important for managing the risks of extreme precipitation events by guiding adaptation and risk mitigation measures, but still remain a major challenge in GCMs.

However, simulating precipitation accurately at global scales is difficult because of the wide range of physical processes involved, from microphysics at the cloud scale to large-scale dynamics of the atmosphere. GCM model simulations are still extremely expensive and time consuming to run, as they need to numerically solve complex partial differential equations describing those processes. This greatly restricts the ability to create large ensemble projections for different climate change scenarios for the next century.

GCMs represent precipitation as diagnostic variable that is computed from the dynamically resolved prognostic atmospheric variables. GCMs need to approximate the atmospheric circulation on discretized grids with coarse spatial resolution. This leads to problems to correctly resolve small-scale dynamics that are important for inferring precipitation. Precipitation is a highly complex process and can not be directly resolved by the coarse GCM, but has to be parameterized. Parameterizations are simplified representations of the subgrid-scale processes that cannot be explicitly resolved due to computational constraints. At each time step, the GCM first solves the atmospheric dynamics, then applies parameterizations to account for subgrid-scale processes like convection and precipitation, updates the atmospheric state, and proceeds to the next step.

Traditional parameterization schemes are mainly column-based approaches that treat each of the discrete vertical GCM grid columns independently. Despite the advancements of column-based methods over the years, they still struggle to accurately capture both fine- and large-scale precipitation patterns, resulting in systematic biases and uncertainties from local to global scales [4–6]. A major simplification that contributes to the biases is that the column-based parameterization neglects local feedback between neighboring columns, which makes it hard to capture mesoscale convective organization. Additionally, the assumed timescales for convection closure can introduce further discrepancies, as convective processes in reality operate on a continuum of timescales that are not well represented in simple quasi-equilibrium closures. The biases show in either over- or underestimation of precipitation intensity and especially in the GCMs ability to represent extreme events. The bias is often especially

pronounced in the tropics, a prominent example being the double Intertropical Convergence Zone (ITCZ) bias [7], where models produce excessive precipitation in the southern tropics.

Small-scale processes that determine precipitation (i.e. cloud microphysics like drop nucleation, accumulation and coalescence) can, for the foreseeable future, not be directly resolved in global ESMs. Also, resolving convection at a global scale seems to remain out of reach for the near future due to rapidly growing computational cost for finer grid spacing. Furthermore, parameterizations rely on tuning based on observed precipitation climatologies, which limits their ability to generalize to changing climate conditions [8].

Both the discretization of atmospheric dynamics and the approximations of column-based parameterizations contribute to significant biases in GCM simulated precipitation. This makes impact assessments and water resource and flood management, which require precise spatial data at high resolution [9], extremely challenging. Also, ensembles of high-resolution precipitation projections are imperative for impact assessments but are currently not available due to computational limitations [8].

Recent studies have shown remarkable success utilizing Deep learning models for weather-forecasting [10–14] and long-term climate simulations [15]. Generative machine learning (ML) methods have been applied for downscaling, bias correction and forecasting tasks, adding the ability to produce ensembles that reflect intrinsic variability [11, 16–19]. Most prominent are generative adversarial networks (GANs) [20] and more recently diffusion models [21]. Diffusion models (DMs) have in recent years often been preferred over GANs because their training is more stable and converges more easily. Also, GANs are prone to suffer from mode collapse, an issue where they are not able to approximate the full distribution, another area where DMs are superior.

There have been efforts using deep learning to replace traditional column-based physical parameterizations in atmospheric models, while preserving the column structure [22–24]. In these approaches, more accurate but very expensive simulations (e.g., cloud-resolving or large-eddy simulations) serve as training data, capturing small-scale processes that standard parameterizations approximate. Neural networks are then trained to emulate complex subgrid-scale physics for much less computational cost. For instance, in ClimSim [25] each atmospheric column can be treated as an independent regression task, mapping one-dimensional state variables to one-dimensional subgrid-scale tendencies. Despite promising results, a central limitation is that as these methods are trained on simulations they inherit biases present in them. As the neural network training is performed under specific climate model conditions, Deep learning (DL) based parameterizations may struggle to generalize to changing climate states in decadal to centennial projections. As the simulations are very expensive, there is limited training data, which can hurt the generalization performance of data-hungry state-of-the-art DL methods. A recent approach [26] combined a fully differentiable dynamical core with a neural network to emulate small scale processes in a hybrid

model setup designed for weather prediction. In a follow up work the authors introduce an additional neural network that infers precipitation rate from the atmospheric column state for a  $2.8^\circ$  grid spacing of satellite-based precipitation [27].

We propose an alternative to column-based parameterizations, a probabilistic ML-based model that directly predicts high-resolution precipitation from low-resolution global atmospheric fields. A notable difference to column-based methods is that ML-based models can act at global scales to capture spatial interactions between various locations and also between different variables. Our model is trained exclusively on the ERA5 reanalysis, which integrates a wide range of observational data through advanced data assimilation techniques within a high-resolution ( $0.25^\circ$ ) weather model. This eliminates the need for emulating expensive small-scale simulations with nested cloud resolving models. Additionally, our proposed approach can also operate as a post-processing tool to derive refined precipitation fields from the atmospheric state once a GCM run has concluded.

We present a two-stage ML framework that operates on a small set of global 2-dimensional atmospheric variables, rather than on individual columns, to produce high-resolution precipitation at  $0.25^\circ$  (Fig. 1). Our goal is to offer a computationally efficient, probabilistic alternative to conventional precipitation parameterizations that comes with less biases and is able to handle climate projections and model extreme events. The framework consists of (I) a global deterministic regression module (UNet) that predicts low-resolution ( $1^\circ$ ) precipitation from a small set of atmospheric variables (near-surface winds, sea-level pressure, and specific humidity), and (II) a conditional diffusion model (DM) that is conditioned on the regression model’s prediction. The DM then generates global fields at  $0.25^\circ$  resolution, capturing fine-scale variability and providing a distribution of possible realizations consistent with the large-scale condition.

The regression model effectively captures the large-scale precipitation response to the atmospheric variables. Meanwhile, the generative diffusion model refines this estimate by removing biases and accurately reconstructing small-scale variability that the regression model alone cannot resolve. As both modules are trained solely on reanalysis data (ERA5), they learn a mapping from a large-scale atmospheric state to precipitation that is not dependent on a specific GCM. We benchmark our model by comparing our precipitation prediction to the ESM4-GFDL model precipitation parameterization. At inference, we use the atmospheric variables of GFDL to get a deterministic precipitation prediction at  $1^\circ$  with our regression model. We use that as input for our DM and predict an ensemble of high-resolution precipitation estimates (at  $0.25^\circ$ ). We add computationally efficient quantile delta mapping (QDM) to correct the regression model’s initial prediction and additionally add noise to those predictions before we condition the DM on the large-scale precipitation fields. Both QDM and adding noise serve the goal of correcting biases inherited from the GFDL atmospheric variables. Adding noise to the conditional-input removes the small-scale variability and allows the model (during training) to learn how to reconstruct small-scales that match the large-scale patterns of the condition at inference.

The key advantages of our approach include:



- **Bias mitigation:** By training our model only on reanalysis and applying our bias corrections, we substantially reduce biases, e.g. in the prominent double ITCZ in GFDL, or in extreme event statistics.
- **Preservation of trends:** Although our approach is trained on historical conditions, we show that it preserves large-scale climate trends (e.g., under SSP3-7.0)
- **Higher-resolution output:** Despite the ESM running at  $1^\circ$  resolution, our DM generates precipitation at  $0.25^\circ$ , providing valuable detail for downstream impact models.
- **Probabilistic ensembles:** The diffusion model offers a way to sample from the conditional precipitation distribution, enabling us to generate ensembles and estimate uncertainty.
- **Speed:** Our model is computationally efficient and needs only about 2 seconds for inferring a global  $0.25^\circ$  precipitation map.

## 2 Results

We first generate a deterministic global precipitation estimation from a small set of atmospheric variables at  $1^\circ$  (Fig. 1A) with our UNet model (Fig. 1B). We apply computationally efficient quantile delta mapping to correct large-scale biases in the regression output to remove biases inherited from the ESM atmospheric variables. We use a conditional DM in the second stage of our approach (Fig. 1C), as the output of the UNet does not correctly model the small-scale variability correctly. Our approach successfully downscales precipitation from  $1^\circ$  to  $0.25^\circ$  resolution in a probabilistic way.

### 2.1 Correction of spatial biases

Comparing the climatologies over 40 years of data shows that GFDL (Fig. ??A) has by far the largest spatial bias, especially showcasing a strong double ITCZ bias, when compared to our regression model (Fig. ??B) and our DM (Fig. ??D). We downsampled both our DM as well as ERA5 from  $0.25^\circ$  to  $1^\circ$  with average pooling for better comparability. To highlight the differences between the climatologies (also at  $1^\circ$ ), we show the difference plots between the precipitation of GFDL and ERA5 (Fig. 2A), our regression model and ERA5 (Fig. 2B) as well as our DM and ERA5 (Fig. 2C). The GFDL parameterization has the highest mean absolute bias of 0.424 mm/d. Our regression model’s precipitation prediction is already an improvement with a bias of 0.129 mm/d. Additionally adding our DM correction to it further, reducing the bias to 0.091 mm/d. The GFDL precipitation is heavily biased in the tropics, either over or underestimating precipitation significantly compared to ERA5. We also compare the climatologies of ERA5 (Fig. ??A) and our DM precipitation (Fig. ??B) at  $0.25^\circ$  high resolution (GFDL is only available at  $1^\circ$ ). The climatologies over 40 years are very similar and only show small differences (Fig. ??C). This is in line with the small mean absolute bias of 0.111 mm/d. Our alternative precipitation estimates and in particular the DM exhibit significantly lower spatial biases compared to the GFDL parameterization at  $1^\circ$ . Our DM has also only a very small spatial bias at the finer  $0.25^\circ$  ERA5-resolution, where GFDL is not available.

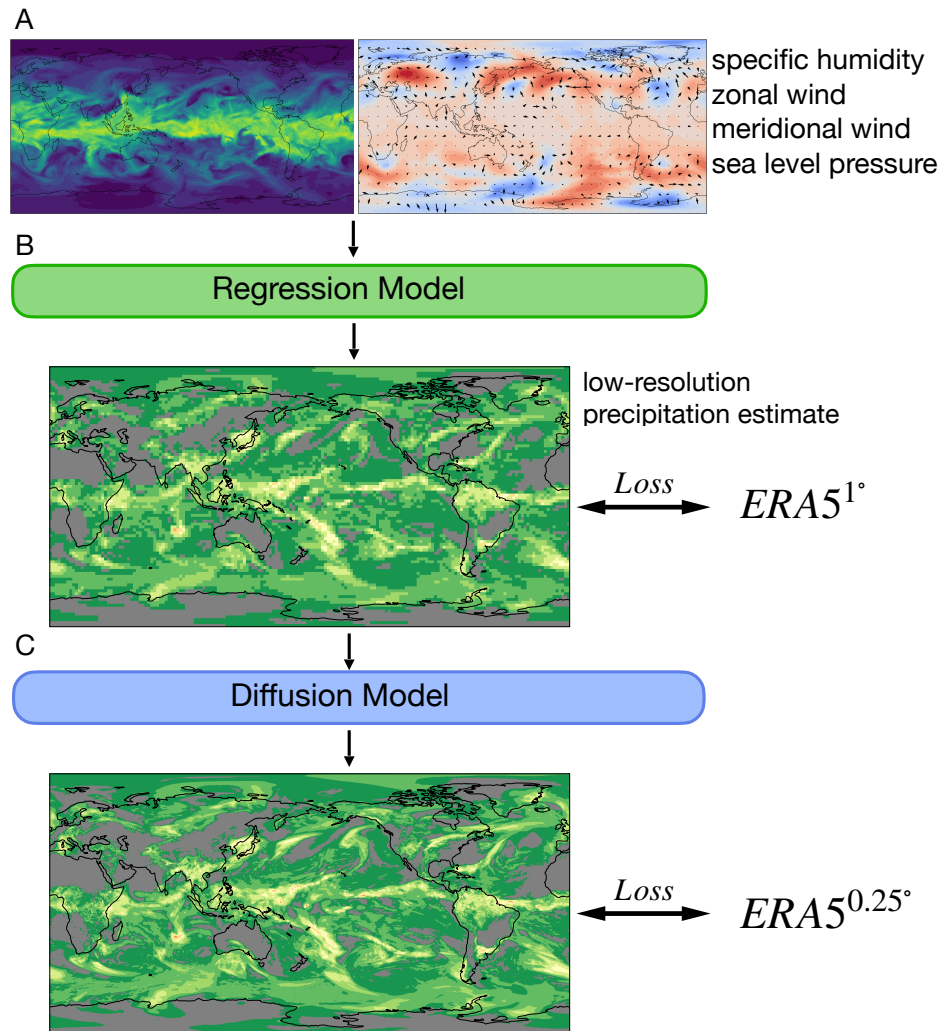


**Fig. 1 Schematic overview of our two-stage approach for generating high-resolution global precipitation from atmospheric variables.** 1) Deterministic UNet Regression Model. We first train a UNet model to learn the mapping from four atmospheric variables at  $1^\circ$  resolution (corresponding to a typical ESM resolution), specific humidity at 850 hPa, near-surface eastward and northward wind components at 10m, and sea-level pressure, to precipitation. During training, both the inputs and the  $1^\circ$  precipitation targets come from ERA5 reanalysis, ensuring the regression model captures the relationship between large-scale atmospheric variables and precipitation. 2) Generative Diffusion Model. We then train a conditional diffusion model to better model the fine-scale spatial structure that are lacking in the regression output. The input to this model are upsampled ( $1^\circ$ ) precipitation fields from ERA5, which we corrupt with noise in order to destroy its small-scale variability. The diffusion model learns to restore these small-scale patterns using high-resolution ( $0.25^\circ$ ) ERA5 precipitation as the training target. At inference we take atmospheric variables from the ESM and apply the trained UNet regression model to generate a deterministic precipitation estimate. Before we use this estimate as a condition for our DM, we apply quantile delta mapping to reduce spatial biases inherited from the biased atmospheric variables of GFDL. The diffusion model is then conditioned on noisy quantile mapped precipitation estimates. By sampling multiple times, we can generate large ensembles of global  $0.25^\circ$  precipitation predictions that are faithful to the large-scale dynamics, yet capture realistic small-scale variability.

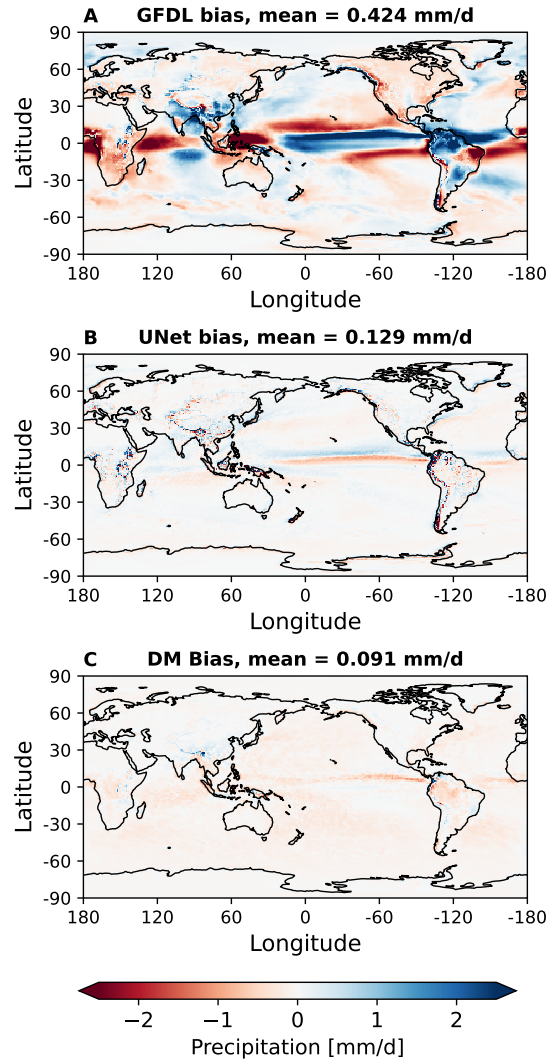


**Fig. 2 Model biases of GFDL, UNET and DM.** The maps show differences in time mean precipitation between ERA5 and (A) GFDL, (B) the UNet regression model, and (C) the DM. The difference map of GFDL shows pronounced bias in the tropical regions, including a double ITCZ. Our regression model alone already improves over GFDL, but the DM leads to further reduced deviations from ERA5 and the smallest mean absolute bias. Note that we downsampled ERA5 and the DM to  $1^\circ$  by applying average pooling for fair comparison to GFDL.

## 2.2 Improving precipitation statistics

The spatial power spectral density (PSD) shows that GFDL struggles to produce variability on small spatial scales that is similar to ERA5 (Fig. 3A). The ESM produces blurry outputs lacking spatial variability at scales up to 400km. At scales between 100km and 400km, our regression model is aligned better with ERA5. Our DM can generate precipitation fields at 0.25° resolution that align well with the spatial spectrum of ERA5, showing its capabilities in correctly modeling spatial variability. The histogram (Fig. 3B) shows that the 1° GFDL model overestimates precipitation between 25 mm/d and 100 mm/d and underestimates precipitation greater than 150 mm/d compared to 0.25° ERA5. Our 1° UNet regression model predicts the precipitation more accurately, but also slightly underestimates the small but more frequent precipitation events with less than 25 mm/d. Our 0.25° DM performs best with only a very slight underestimation of extreme events with more than 150 mm/d, similar to the regression model. For the latitudinal and longitudinal mean comparisons (Fig. 3C and Fig. 3D), we bi-linearly interpolated the regression model and GFDL precipitation to 0.25°. Both plots show that both of our proposed models align well with the ERA5 statistics, while GFDL sometimes deviates significantly, depending on the region. The differences between the DM, UNet and GFDL compared to ERA5 are further highlighted in Fig. ??.

## 2.3 Reproducing extreme events

To assess whether our diffusion model (DM) can adequately reproduce present-day climate extremes and adapt to unobserved future conditions, we compare the R95p extreme precipitation index across historical and projected climates under SSP3-7.0 (Fig. ??).

We compute the annual total precipitation from days exceeding the 95th percentile (R95p index) to compare historical extreme precipitation of ERA5 and (Fig. 4A - Fig. 4D) our UNet regression model, GFDL and our DM.

During the historical period (1980–2005), GFDL exhibits pronounced biases in the mid-latitudes and tropics, including a double ITCZ bias, leading to an overestimation of extreme rainfall around the equator (Fig. ??B). Our ML models follow ERA5 closely, exhibiting smaller deviations in both spatial extent and magnitude. The DM in particular reduces the wet bias of GFDL effectively, and is more closely aligned with ERA5. The reference period for the computation is 1980–2020.

Under the future warming scenario SSP3-7.0 (between 2075–2100), all models predict an increase in R95p in the tropics relative to the historical period (Fig. ??D – Fig. ??F). Because model biases can alter the magnitude of these changes, we compare the sign of the change across the plots, which is largely consistent among GFDL, UNet regression, and DM. Overall, GFDL exhibits the strongest intensification of precipitation, while the DM and UNet produce a more moderate increase, with some regional disagreements, particularly over South America. The double ITCZ bias remains visible in the future projections of GFDL. Visually, both GFDL and DM show stronger extremes within the tropical belt, although GFDL changes are larger in magnitude overall, possibly reflecting its known wet bias. Our DM reproduces

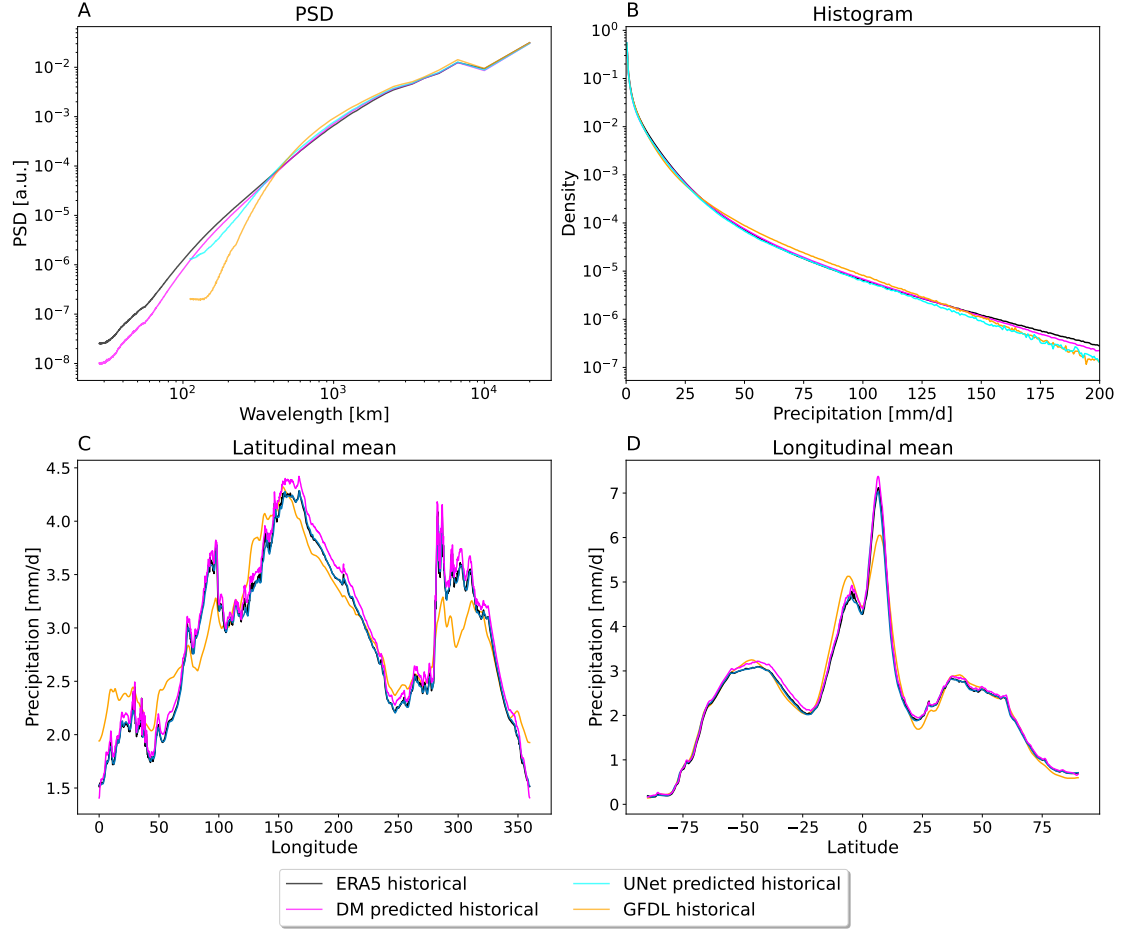


**Fig. 3** Reproduction of the statistics of ERA5 at  $0.25^\circ$  resolution over 40 years. **(A)** Mean spatial power spectral density (PSD). The diffusion model corrects the small-scale spatial details and follows the target distribution closely. **(B)** Histogram indicating the precipitation frequencies. The histogram also shows large improvements with slight deviations from the ERA5 reference data at  $0.25^\circ$  resolution for extreme precipitation. **(C)** Longitude profile, given by the data averaged over all longitudes, weighted by the cosine of latitude to account for the varying grid cell area. **(D)** Latitude profile, given by the data averaged over all longitudes. Our diffusion model approximates the latitude and longitude profile of the original ERA5 reference data well. For panels (B-C), we bi-linearly upsample the GFDL and our regression model predictions of precipitation (orange/cyan) from  $1^\circ$  to the  $0.25^\circ$  resolution of ERA5 and the DM.

similar spatial patterns (signs of change) but with a more modest amplitude, suggesting that it partially corrects the climatological biases of GFDL, while retaining the overarching signal of climate change.

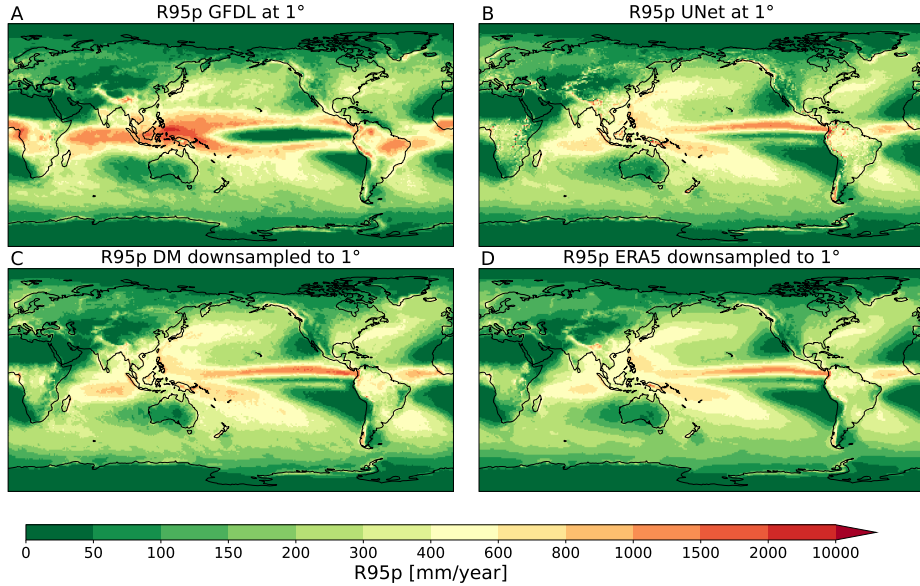


**Fig. 4 Evaluation of extreme event coverage for the historical period. (A-D):** Climatology of R95p (annual total precipitation from days exceeding the 95th percentile) for the historical period simulated by (A) UNet at  $1^\circ$ , (B) GFDL at  $1^\circ$ , and (C) the Diffusion Model (DM) downsampled to  $1^\circ$ , compared to (D) ERA5 reanalysis downsampled to  $1^\circ$ . The GFDL model exhibits strong wet biases in the tropics (A), whereas the DM and UNet models show reduced biases (E, G), aligning well with the spatial patterns of ERA5.

We further evaluate extreme-event performance by comparing consecutive wet days (CWD) and consecutive dry days (CDD) during the historical period (1980-2005) against ERA5 (Fig.??). The largest differences tend to appear over the tropics, where pronounced convective precipitation leads to larger deviations in CWD, and over subtropical regions where prolonged dry periods cause sizable shifts in CDD. Both our ML-based approaches, but especially the diffusion model, capture ERA5 patterns of CWD and CDD more accurately, clearly improving upon the biases of GFDL.

## 2.4 Ensemble evaluation

A key strength of our generative DM parameterization over traditional column-based parameterization is its ability to generate a diverse ensemble of possible high-resolution precipitation realizations for a given low-resolution condition. It is critical to evaluate the internal variability of our diffusion model in the downscaling task. We investigate whether the uncertainty in a DM ensemble aligns with the inherent uncertainty of downscaling the data from  $1^\circ$  to  $0.25^\circ$ . Note that the diffusion model also performs bias correction by regenerating noisy small-scale variability. We condition our DM on a given noisy low-resolution ERA5 validation year and evaluate the model 50 times for each day in the year, resulting in a 50-member DM ensemble of one-year trajectories.

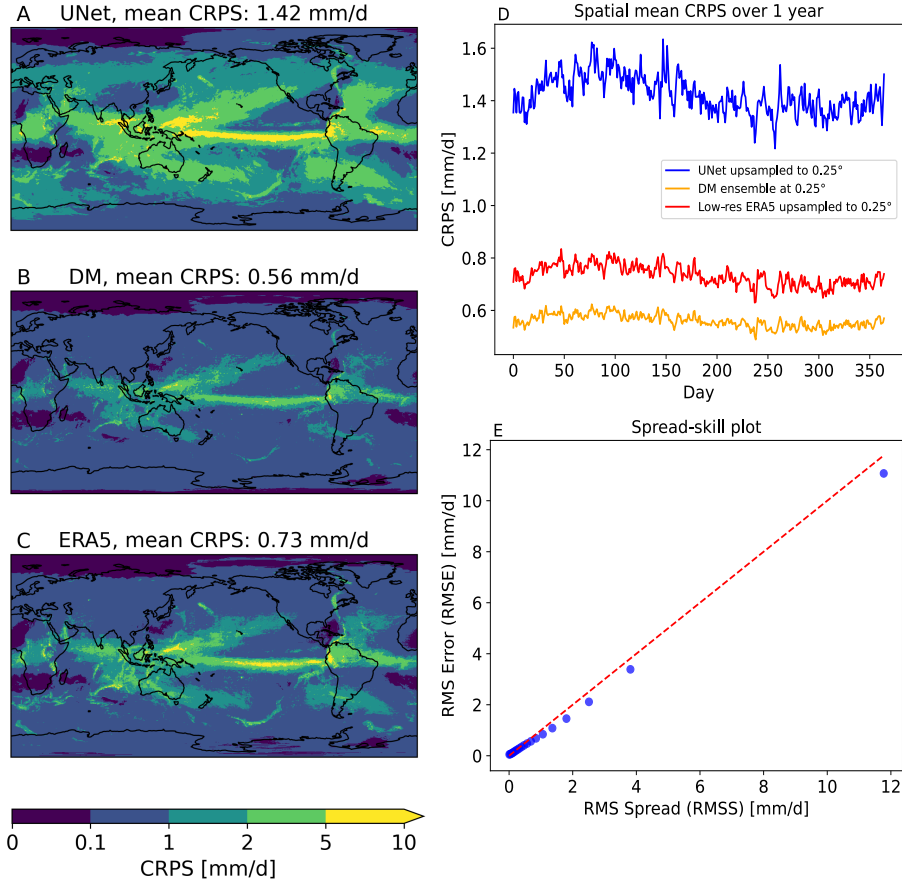


**Fig. 5 Evaluation of the 50 DM ensemble members over one reference ERA5 year.** Temporally averaged continuous ranked probability score (CRPS) (lower is better) for (A) applying our deterministic UNet and then bi-linearly interpolating to 0.25°, (B) our DM and (C) the bi-linearly upsampled deterministic ERA5 baseline. Our DM achieves the lowest CRPS overall. (D) shows that our DM also maintains the lowest spatially averaged CRPS throughout the year. (E) The spread-skill plot indicates that our DM closely follows the 1:1 line, demonstrating well-calibrated spread of the DM model with respect to the underlying uncertainties.

The downscaling ground truth will be the respective high-resolution ERA5 year. We compare the continuous ranked probability score (CRPS) [28] of our 50-member DM downscaling with bi-linearly upsampled low-resolution (LR) ERA5 and bi-linearly upsampled precipitation predicted by the regression model. This comparison assesses how well the DM’s ensemble spread matches the inherent uncertainty.

Our DM outperforms both deterministic baselines in terms of temporally averaged CRPS (Fig. 5A - Fig. 5C). The mean CRPS of our DM is the lowest with 0.56 mm/day, better than the ERA5 upsampled from 1° to 0.25° (0.73 mm/day) and the upsampled



UNet prediction (1.42 mm/day). The spatially averaged CRPS (Fig. 5D) also shows that our model has the best scores overall. The spread-skill of our model roughly follows the 1:1 line, indicating an accurate, well-calibrated representation of uncertainty (Fig. 5E). For larger spreads the RMSE is slightly too low (underconfident).

## 2.5 Precipitation generation for climate projections

In the following, we apply our ML method to future climate projections. This is a challenging task, given that the underlying distribution shifts over time in response to changing climate conditions. A comparison between our regression and the diffusion model (Fig. ??) for SSP3-7.0 data between 2015-2100 shows that our DM is still able to increase the spatial resolution of the precipitation predictions from  $1^\circ$  to  $0.25^\circ$  with ERA5-like large-scale patterns and only slight deviations on the small scales (Fig. ??A).

### Trend preservation

We tested the ability of our diffusion model to extrapolate to an unseen future climate scenario, namely SSP3-7.0, which projects relatively high greenhouse gas emissions and therefore increasing specific humidity. First, we initialize our regression model with the SSP3-7.0 atmospheric variables and then apply quantile delta mapping. We find that the regression model forecasts an increasing precipitation trend, driven largely by the higher specific humidity (Fig. 6). The spatial trend at each location (Fig. ??A - Fig. ??C) reveals that applying the DM on the UNet precipitation preserves the spatial patterns of the trend. While the spatial patterns are similar, the DM corrects the local structures and intensities. The spatial trends predicted by the regression model differ in sign from the GFDL projections in some regions. The spatially averaged annual mean trend reveals that the UNet regression model has a different annual mean precipitation and exhibits an overly large variance, resulting in a too large trend. When we correct the regression models precipitation with our DM, the model adjusts the mean and variance such that the annual precipitation trend matches the trend of the GFDL SSP3-7.0 projection more closely (Fig. 6). After applying the DM, there is only a small deviation in the globally averaged mean values and trend compared to the GFDL projection. It is important to note that the GFDL trend is also not a strict ground truth. Our DM robustly adapts to future climate scenarios by preserving large-scale structures while allowing consistent ERA5-like small-scale variability. This combination allows to correct spatial patterns while preserving the global trend information, even when the distributions of the atmospheric variables change. Although SSP3-7.0 can be seen as an out-of-distribution test in terms of temperature increases, in practice it represents a moderate distribution shift for precipitation, i.e., mostly an increase in the frequency of higher humidity values rather than entirely novel conditions outside the historical range.

### Spatial climate change signal

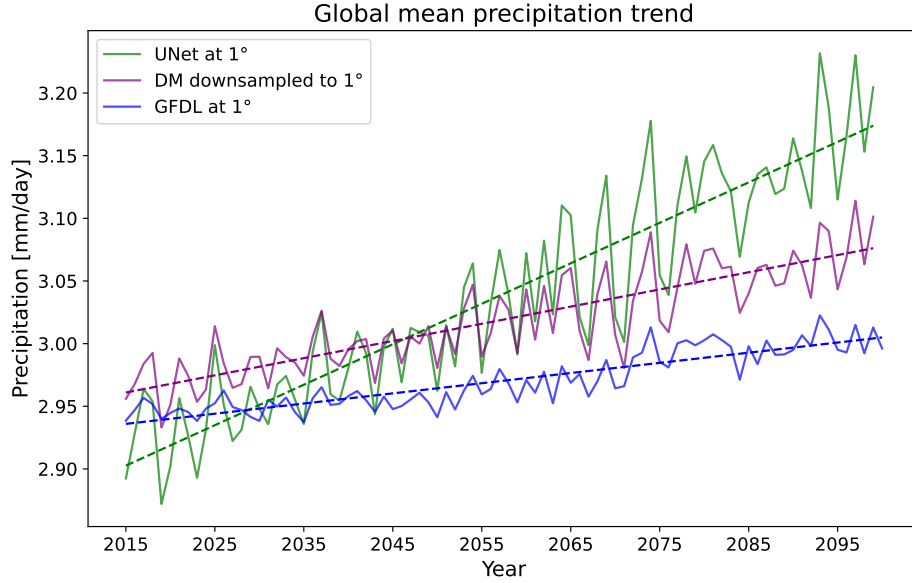


**Fig. 6 Our DM reproduces the GFDL trend under the SSP3-7.0 scenario.** Comparison of globally and annually averaged precipitation trends for the SSP3-7.0 scenario for GFDL (blue), our regression model (green) and our DM (purple). The spatial and globally averaged trend of the UNet (even after quantile delta mapping) is different to GFDL. The DM adjusts the UNet trend by regenerating new small-scale variability. The DM corrects the global average trend of the UNet, aligning it more with GFDL. The DM trend is slightly larger than that of GFDL, while the mean values are slightly lower. Note that the GFDL trend is not a strict ground truth but rather serves as a reference for comparison, as the DM performs a correction of the data towards the ERA5 distribution. Our model effectively captures and reproduces precipitation trends from the change signal in both the circulation variables and the specific humidity.

Fig. ?? shows the relative signal of climate change in precipitation (2075-2100 vs. 1980-2005) relative to the historical period for GFDL (Fig. ??A), the UNet regression model (Fig. ??B), and our Diffusion Model (Fig. ??C). Overall, both UNet and DM capture large-scale changes while offering more moderate local responses than GFDL. In the tropics and especially the ITCZ region, GFDL exhibits a stronger positive precipitation response compared to both data-driven methods, which generally temper the climate change signal. In particular, in parts of South America, the sign of the projected change switches from positive in GFDL to almost zero or slightly negative for the UNet and DM. As we show that the overall trend of precipitation is well approximated in statistical metrics and time series trends, this could suggest that the ML-based models correct for some of the potential biases of GFDL, resulting in different and in some cases opposite regional precipitation trends.

### 3 Discussion

We introduced a two-stage framework composed of a deterministic UNet regression model together with a probabilistic conditional diffusion model for inferring high-resolution global precipitation fields from a small set of atmospheric atmospheric variables. Our generative Machine Learning approach hence provides a spatial-pattern-aware alternative to column-based parameterization of precipitation for ESMs.

A key advantage of our approach is that both our models are trained exclusively on ERA5 reanalysis data. This independence from any particular ESM means that our method can be applied to any ESM without any retraining. The only parameter in the training that depends on the ESM is the amount of noise we should add to the DM’s condition, which could slightly vary for ESMs different from GFDL. Not changing the noise-scale could potentially result in only incomplete removal of small-scale biases in models where the spatial scales are resolved worse than in GFDL. Most of the bias will, however, still be removed by QDM and the DM.

Another advantage of our framework is its computational efficiency. With inference times of roughly two seconds per global  $0.25^\circ$  precipitation prediction, our model is a fast alternative to column-based parameterizations.

Our approach efficiently produces ensembles of high-resolution precipitation fields from low-resolution atmospheric variables, which faithfully represent the inherent uncertainty in the downscaling process. Our method can also be used in post-processing for generating large ensembles and long-term precipitation projections, which are essential for impact and risk assessments.

Our evaluation demonstrates that our method significantly reduces the bias compared to our ESM reference. Our approach successfully avoids the prominent double ITCZ bias which is strongly pronounced in the GFDL model. Our method also reproduces accurate small-scale spatial patterns with which ESMs often struggle. In the power spectral density we confirm that the small-scale spatial variability of the downscaled precipitation aligns closely with the ERA5 reanalysis data taken as ground truth, which is a big improvement over the blurry GFDL precipitation fields. The spatial variability of small scales is essential for accurate simulation of regional precipitation extremes and associated impact assessments.

Importantly, our framework preserves the climate change signal inherent in the specific humidity under the SSP3-7.0 scenario, while correcting small-scale spatial patterns in accordance to reanalysis data. Compared to the UNet, our diffusion model more effectively adjusts the spatial variability of precipitation, bringing it closer in line with the GFDL projections, while the global mean remains slightly different. This deviation reflects the fact that GFDL is not treated as ground truth in our setup and the diffusion model performs a bias correction toward ERA5, balancing consistency with climate model trends and alignment with observational data. In contrast, our UNet regression model alone fails to reproduce the mean and predicts too much variance. An essential part of our method is to add noise to the regression model’s  $1^\circ$  output before conditioning the diffusion model on it. This removes the

flawed small-scale features while preserving large-scale dynamics, effectively acting as a bias correction for the small-scales. We show that the spatial features indicating an increase and decrease in the trend of the UNet output are preserved by our DM. By regenerating improved, reanalysis-like, small-scale structures the DM aligns the global, spatially averaged, trend with the trend of the GFDL projection, reducing the precipitation intensities of the UNet predictions. Our model demonstrates robustness to out-of-distribution scenarios as shown by its ability to preserve trends and capture extreme events under the SSP3-7.0 scenario.

An important practical benefit of our model producing  $0.25^\circ$  resolution is that it enables coupling the precipitation outputs to impact or land models without requiring a higher resolution for the  $1^\circ$  atmospheric variables. This decoupling of scales can substantially lower computational costs while still providing the detailed precipitation fields needed for impact studies.

Still, several avenues for future research remain. An immediate extension is to integrate our DM-based parameterization directly into a climate model and evaluate its stability in a fully coupled system. Such experiments can help determine whether further constraints on the UNet outputs are necessary when deployed in operational settings. This includes physical constraints to assure that physical conservation laws are fulfilled. Optimizing the inference strategy with techniques such as model distillation [29] could be explored to accelerate the sampling process and further reduce computational cost.

## 4 Methods

Our approach consists of two models, a deterministic regression model and a probabilistic diffusion model (Fig. 1). Both models are trained purely on ERA5 reanalysis data between 1980-2018. We first train a UNet regression model to predict a global precipitation estimate at  $1^\circ$  spatial resolution. The inputs to this UNet are  $1^\circ$  fields of specific humidity at 850 hPa, sea level pressure, and near-surface wind components (eastward and northward at 10 m), while the target variable is the precipitation of ERA5. When applying the trained UNet to historical or SSP3-7.0 scenario atmospheric variables derived from GFDL, we perform Quantile Delta Mapping (QDM) to provide a cost-effective bias correction. This correction step mitigates systematic biases introduced by GFDL atmospheric variables, preventing those biases from propagating into the final precipitation predictions.

The second component of our framework is a probabilistic conditional diffusion model, which is trained to produce high-resolution ( $0.25^\circ$ ) precipitation fields. It serves two purposes: (I) downscaling from  $1^\circ$  to  $0.25^\circ$  resolution, and (II) correcting small-scale spatial biases. For downscaling, we condition on low-resolution ( $1^\circ$ ) ERA5 fields that have been bilinearly upsampled to match the number of pixels in the high-resolution grid ( $720 \times 1440$  pixel). To correct small-scale biases, we first remove information below a chosen spatial scale by injecting noise, thus effectively replaces the small-scale patterns with noise. We effectively achieve a small-scale bias correction by letting the model generate new information for those noised scales. The small scales generated by the DM are consistent with the large scales that were unaffected by the noise. There is a direct relationship between the noise injected and the spatial scales that are corrupted by the noise [16], adding more noise destroys information up to larger scales. Even after applying quantile mapping (QM) to the precipitation predicted by our regression model, we still observe discrepancies in the power spectra compared to high-resolution ERA5 data. In particular, the regression model tends to underestimate small-scale variability. To compensate for this, we add noise to the fields in order to remove the biased small-scale spatial patterns in the regression model output. Both QM and the noise injection step act as bias correction measures in our framework. QM addresses large-scale biases efficiently but does not fully resolve small-scale variability, while noising the diffusion models condition allows the DM to regenerate more realistic small-scale structures, consistent with the bias-corrected large scales.

By first applying our regression model to the atmospheric variables, we obtain a deterministic precipitation estimate. This estimate then serves as the condition for our conditional diffusion model, which generates a high-resolution ensemble of precipitation fields that match the atmospheric variables. We remove biases inherited from the atmospheric variables by first applying quantile delta mapping (QDM) to the deterministic precipitation estimation and then removing the small-scale variability when conditioning the DM on it. The DM generates reanalysis-like small-scale patterns that are consistent with the large-scales predicted from atmospheric variables.

## 4.1 Setup: Regression model

We first train a deterministic UNet model at a global  $1^\circ$  resolution to infer precipitation from a small set of atmospheric variables. We train the regression model on ERA5 reanalysis data, with specific humidity at 850 hPa, sea level pressure, and near-surface wind components (eastward and northward at 10 m) as input and precipitation as target. Training on reanalysis data allows the model to learn the relationship between atmospheric variables and precipitation. This is preferable over training it on ESM data, where the model would learn a heavily biased relationship resulting from the models precipitation parameterization. At inference, we directly input the atmospheric variables of GFDL into the trained model. The resulting precipitation inherits some of the biases that the GFDL atmospheric variables contain. To mitigate this bias, we apply a computationally efficient quantile delta mapping step as post-processing on the UNet output.

## 4.2 Noising setup Diffusion model

We train a generative conditional diffusion model to produce high-resolution precipitation that resembles reanalysis data, given a low-resolution precipitation condition. Training the diffusion model directly on ESM data would introduce ESM-inherent biases, so we instead train on ERA5 reanalysis exclusively. Because the ESM and ERA5 data are not paired, we cannot establish direct conditioning between them during training. During training, we can therefore only condition the model on reanalysis data. As a result, the DM is trained using ERA5 as both the condition (low-resolution input) and the target (high-resolution output). At inference, we want to condition the DM on ESM precipitation. To ensure that the model generalizes well, the distribution of the conditional data during inference must match the conditional data distribution during training. During inference, we add noise to the regression model’s  $1^\circ$  output to remove flawed small-scale variability; therefore, during training, we ensure consistency by conditioning the diffusion model on downsampled  $1^\circ$  ERA5 fields with the same noise level. This added noise destroys small-scale variability in the LR ERA5 data up to the point in the power spectrum density (PSD), where the spectrum of ERA5 and our regression models precipitation estimate start to diverge. The small scales of the training and inference conditions will therefore be identical, both dominated by noise. More details on how the noise level is chosen can be found in [16].

In summary, we train the DM to produce high-resolution ( $0.25^\circ$ ) ERA5 data from noisy low-resolution ( $1^\circ$ ) ERA5 data. The training is independent of any ESM data. During inference, we use the precipitation estimate of our regression model at  $1^\circ$  as condition for the DM. We first apply a quantile delta mapping bias correction and then add the same level of noise used during training (to match the PSD’s). This approach ensures that training and inference condition inputs are distributed similarly, allowing our DM to generalize effectively.

### 4.3 Network architecture and training

Our regression model, which provides a deterministic estimate of precipitation from large-scale atmospheric variables, follows a memory-efficient design [30]. Specifically, the UNet has four input channels, one channel per atmospheric variable, and one output channel for precipitation. We increase the feature dimension across four stages using multipliers of (1,2,2,2), incorporating a ResNet block at each stage, and include only a single bottleneck attention layer to keep computational demand minimal. The model is trained for 2000 epochs with the Adam optimizer [31], using a learning rate of  $1e^{-4}$ .

Our diffusion model builds upon a Denoising Diffusion Probabilistic Model (DDPM) [21], conditioned on coarse-resolution images. We employ state-of-the-art techniques to facilitate faster convergence. The U-Net follows the  $180 \times 360 \rightarrow 720 \times 1440$  Efficient U-Net [30] architecture, that we also use in our regression model. The diffusion model architecture utilizes a cosine schedule for noising the target data and a linear schedule for the condition during noise condition augmentation. The diffusion model is trained for 1100 epochs using the ADAM optimizer [31] with a batch size of 1 and a learning rate of  $1e^{-4}$ . We train the model using 1000 noising steps. We use 1000 noising steps during training but reduce this to 100 steps at inference to significantly decrease sampling time while maintaining high-quality outputs.

### 4.4 Data

During both training and inference, we use the same four prognostic variables: specific humidity at 850 hPa, eastward and northward wind components at 10m, and sea level pressure. The target data is always daily total precipitation.

#### ERA5

ERA5 [32] is a state-of-the-art atmospheric reanalysis dataset provided by the European Center for Medium-Range Weather Forecasting (ECMWF). ERA5 data was downloaded from [https://developers.google.com/earth-engine/datasets/catalog/ECMWF\\_ERA5\\_DAILY?hl=de#colab-python](https://developers.google.com/earth-engine/datasets/catalog/ECMWF_ERA5_DAILY?hl=de#colab-python). The training period comprises ERA5 data from 1980-01-01 to 2018-05-02, for evaluation it is 2018-05-03 to 2020-07-09.

#### GFDL

The ESM data we use is from GFDL-ESM4 [33], a member of Phase 6 of the Coupled Model Intercomparison Project (CMIP6). The historical period spans 1970-01-01 to 2014-12-31. For evaluating our models performance under future projections, we use GFDL-ESM4 SSP3-7.0 from 2015-01-01 to 2100-12-31.

### Data pre-processing

The precipitation units of the GFDL data are  $\text{kg m}^{-2}\text{s}^{-1}$ , and for ERA5 m/h. For consistency, both are transformed to mm/d.

Our pre-processing pipeline of the precipitation data consists of:

- Only GFDL: rescaling the original  $1^\circ \times 1.25^\circ$  GFDL data to  $1 \times 1^\circ$ .
- Add +1 mm/d precipitation to each value in order to be able to apply a log-transformation to the data.
- Apply the logarithm with base 10 in order to compress the range of values.
- Standardize the data, i.e. subtract the mean and divide by the standard deviation to facilitate training convergence.
- Transform the data to the range [-1,1] to facilitate the convergence of the training.

The UNet model is trained on  $1^\circ$  ERA5 data and applied to  $1^\circ$  GFDL data. We generate the  $1^\circ$  ERA5 data by downsampling, only keeping every fourth pixel in the high-resolution data. The downsampling blocks in the UNet model further require padding of the input to 192x368 pixel. For GFDL data, we apply quantile delta mapping (QDM [34]) with 500 quantiles to the predictions that the UNet outputs.

For the condition of the DM, both  $1^\circ$  GFDL and ERA5 data with 180x360 pixels are bilinearly upsampled to match the 720x1440 pixel count of  $0.25^\circ$  target data. Note that originally the  $0.25^\circ$  would have 721x1440 pixel but we leave out 1 row to avoid padding the UNet in the diffusion model.

The preprocessing for the atmospheric variables comprises:

- Standardizing the data, i.e. subtracting the mean and dividing by the standard deviation to facilitate training convergence.
- Transforming the data to the range [-1,1] to facilitate the convergence of the training.



## References

- [1] H. Lee, K. Calvin, D. Dasgupta, G. Krinner, A. Mukherji, P. Thorne, C. Trisos, J. Romero, P. Aldunce, K. Barret, G. Blanco, W. W. Cheung, S. L. Connors, F. Denton, A. Diongue-Niang, D. Dodman, M. Garschagen, O. Geden, B. Hayward, C. Jones, F. Jotzo, T. Krug, R. Lasco, Y.-Y. Lee, V. Masson-Delmotte, M. Meinshausen, K. Mintenbeck, A. Mokssit, F. E. Otto, M. Pathak, A. Pirani, E. Poloczanska, H.-O. Pörtner, A. Revi, D. C. Roberts, J. Roy, A. C. Ruane, J. Skea, P. R. Shukla, R. Slade, A. Slangen, Y. Sokona, A. A. Sörensson, M. Tignor, D. van Vuuren, Y.-M. Wei, H. Winkler, P. Zhai, Z. Zommers, J.-C. Hourcade, F. X. Johnson, S. Pachauri, N. P. Simpson, C. Singh, A. Thomas, E. Totin, P. Arias, M. Bustamante, I. Elgizouli, G. Flato, M. Howden, C. Méndez-Vallejo, J. J. Pereira, R. Pichs-Madruga, S. K. Rose, Y. Saheb, R. S. Rodríguez, D. Ürge-Vorsatz, C. Xiao, N. Yassaa, A. Alegría, K. Armour, B. Bednar-Friedl, K. Blok, G. Cissé, F. Dentener, S. Eriksen, E. Fischer, G. Garner, C. Guivarch, M. Haasnoot, G. Hansen, M. Hauser, E. Hawkins, T. Hermans, R. Kopp, N. Leprince-Ringuet, J. Lewis, D. Ley, C. Ludden, L. Niamir, Z. Nicholls, S. Some, S. Szopa, B. Trewin, K.-I. van der Wijst, G. Winter, M. Witting, A. Birt, M. Ha, J. Romero, J. Kim, E. F. Haites, Y. Jung, R. Stavins, A. Birt, M. Ha, D. J. A. Orendain, L. Ignon, S. Park, and Y. Park, “Ipcc, 2023: Climate change 2023: Synthesis report, summary for policymakers. contribution of working groups i, ii and iii to the sixth assessment report of the intergovernmental panel on climate change [core writing team, h. lee and j. romero (eds.)]. ipcc, geneva, switzerland.” Technical Report 10.59327/IPCC/AR6-9789291691647.001, Intergovernmental Panel on Climate Change (IPCC), Geneva, Switzerland, 2023. Please access report for extended list of writing team, editors, scientific steering committee and other contributing authors.
- [2] A. F. Prein, R. M. Rasmussen, K. Ikeda, C. Liu, M. P. Clark, and G. J. Holland, “The future intensification of hourly precipitation extremes,” *Nature climate change*, vol. 7, no. 1, pp. 48–52, 2017.
- [3] F. V. Davenport, M. Burke, and N. S. Diffenbaugh, “Contribution of historical precipitation change to us flood damages,” *Proceedings of the National Academy of Sciences*, vol. 118, no. 4, p. e2017524118, 2021.
- [4] T. Schneider, J. Teixeira, C. S. Bretherton, F. Brient, K. G. Pressel, C. Schär, and A. P. Siebesma, “Climate goals and computing the future of clouds,” *Nature Climate Change*, vol. 7, no. 1, pp. 3–5, 2017.
- [5] E. M. Wilcox and L. J. Donner, “The frequency of extreme rain events in satellite rain-rate estimates and an atmospheric general circulation model,” *Journal of Climate*, vol. 20, no. 1, pp. 53–69, 2007.
- [6] M. J. Webb, F. H. Lambert, and J. M. Gregory, “Origins of differences in climate sensitivity, forcing and feedback in climate models,” *Climate Dynamics*, vol. 40, pp. 677–707, 2013.
- [7] Y.-T. Hwang and D. M. Frierson, “Link between the double-intertropical convergence zone problem and cloud biases over the southern ocean,” *Proceedings of the National Academy of Sciences*, vol. 110, no. 13, pp. 4935–4940, 2013.
- [8] S. Bordoni, S. M. Kang, T. A. Shaw, *et al.*, “The futures of climate modeling,”

- npj Climate and Atmospheric Science*, vol. 8, p. 99, 2025.
- [9] E. Gutmann, T. Pruitt, M. P. Clark, L. Brekke, J. R. Arnold, D. A. Raff, and R. M. Rasmussen, “An intercomparison of statistical downscaling methods used for water resource assessments in the united s tates,” *Water Resources Research*, vol. 50, no. 9, pp. 7167–7186, 2014.
  - [10] K. Bi, L. Xie, H. Zhang, X. Chen, X. Gu, and Q. Tian, “Accurate medium-range global weather forecasting with 3d neural networks,” *Nature*, vol. 619, no. 7970, pp. 533–538, 2023.
  - [11] I. Price, A. Sanchez-Gonzalez, F. Alet, T. R. Andersson, A. El-Kadi, D. Masters, T. Ewalds, J. Stott, S. Mohamed, P. Battaglia, *et al.*, “Probabilistic weather forecasting with machine learning,” *Nature*, vol. 637, no. 8044, pp. 84–90, 2025.
  - [12] R. Lam, A. Sanchez-Gonzalez, M. Willson, P. Wirnsberger, M. Fortunato, F. Alet, S. Ravuri, T. Ewalds, Z. Eaton-Rosen, W. Hu, *et al.*, “Learning skillful medium-range global weather forecasting,” *Science*, vol. 382, no. 6677, pp. 1416–1421, 2023.
  - [13] C. Bodnar, W. P. Bruinsma, A. Lucic, M. Stanley, J. Brandstetter, P. Garvan, M. Riechert, J. Weyn, H. Dong, A. Vaughan, *et al.*, “Aurora: A foundation model of the atmosphere,” *arXiv preprint arXiv:2405.13063*, 2024.
  - [14] M. Chantry, S. Lang, M. Alexe, J. Dramsch, B. Raoult, M. Clare, M. Santa Cruz, S. Hahner, R. Adewoyin, F. Pinault, *et al.*, “Aifs-ecmwf’s data-driven forecasting system,” in *105th AMS Annual Meeting*, AMS, 2025.
  - [15] O. Watt-Meyer, G. Dresdner, J. McGibbon, S. K. Clark, J. Duncan, B. Henn, M. Peters, N. D. Brenowitz, K. Kashinath, M. Pritchard, B. Bonev, and C. Bretherton, “Ace: A fast, skillful learned global atmospheric model for climate prediction,” in *NeurIPS 2023 Workshop on Tackling Climate Change with Machine Learning*, 2023.
  - [16] M. Aich, P. Hess, B. Pan, S. Bathiany, Y. Huang, and N. Boers, “Conditional diffusion models for downscaling & bias correction of earth system model precipitation,” *arXiv preprint arXiv:2404.14416*, 2024.
  - [17] P. Hess, M. Aich, B. Pan, and N. Boers, “Fast, scale-adaptive, and uncertainty-aware downscaling of earth system model fields with generative foundation models,” *arXiv e-prints*, pp. arXiv-2403, 2024.
  - [18] H. Addison, E. Kendon, S. Ravuri, L. Aitchison, and P. A. Watson, “Machine learning emulation of a local-scale uk climate model,” *arXiv preprint arXiv:2211.16116*, 2022.
  - [19] P. Hess, M. Drüke, S. Petri, F. M. Strnad, and N. Boers, “Physically constrained generative adversarial networks for improving precipitation fields from earth system models,” *Nature Machine Intelligence*, vol. 4, no. 10, pp. 828–839, 2022.
  - [20] I. Goodfellow, J. Pouget-Abadie, M. Mirza, B. Xu, D. Warde-Farley, S. Ozair, A. Courville, and Y. Bengio, “Generative adversarial networks,” *Communications of the ACM*, vol. 63, no. 11, pp. 139–144, 2020.
  - [21] J. Ho, A. Jain, and P. Abbeel, “Denoising diffusion probabilistic models,” *Advances in neural information processing systems*, vol. 33, pp. 6840–6851, 2020.
  - [22] S. Rasp, M. S. Pritchard, and P. Gentine, “Deep learning to represent subgrid processes in climate models,” *Proceedings of the national academy of sciences*,

- vol. 115, no. 39, pp. 9684–9689, 2018.
- [23] P. Gentine, M. Pritchard, S. Rasp, G. Reinaudi, and G. Yacalis, “Could machine learning break the convection parameterization deadlock?,” *Geophysical Research Letters*, vol. 45, no. 11, pp. 5742–5751, 2018.
- [24] J. Yuval and P. A. O’Gorman, “Stable machine-learning parameterization of subgrid processes for climate modeling at a range of resolutions,” *Nature communications*, vol. 11, no. 1, p. 3295, 2020.
- [25] S. Yu, W. Hannah, L. Peng, J. Lin, M. A. Bhourri, R. Gupta, B. Lütjens, J. C. Will, G. Behrens, J. Busecke, *et al.*, “Climsim: A large multi-scale dataset for hybrid physics-ml climate emulation,” *Advances in Neural Information Processing Systems*, vol. 36, pp. 22070–22084, 2023.
- [26] D. Kochkov, J. Yuval, I. Langmore, P. Norgaard, J. Smith, G. Mooers, M. Klöwer, J. Lottes, S. Rasp, P. Düben, *et al.*, “Neural general circulation models for weather and climate,” *Nature*, vol. 632, no. 8027, pp. 1060–1066, 2024.
- [27] J. Yuval, I. Langmore, D. Kochkov, and S. Hoyer, “Neural general circulation models optimized to predict satellite-based precipitation observations,” *arXiv preprint arXiv:2412.11973*, 2024.
- [28] H. Hersbach, “Decomposition of the continuous ranked probability score for ensemble prediction systems,” *Weather and Forecasting*, vol. 15, no. 5, pp. 559–570, 2000.
- [29] E. Luhman and T. Luhman, “Knowledge Distillation in Iterative Generative Models for Improved Sampling Speed,” Jan. 2021. arXiv:2101.02388 [cs].
- [30] C. Saharia, W. Chan, S. Saxena, L. Li, J. Whang, E. L. Denton, K. Ghasemipour, R. Gontijo Lopes, B. Karagol Ayan, T. Salimans, J. Ho, D. Fleet, and M. Norouzi, “Photorealistic text-to-image diffusion models with deep language understanding,” *Advances in neural information processing systems*, vol. 35, pp. 36479–36494, 2022.
- [31] D. Kingma and J. Ba, “Adam: A method for stochastic optimization,” in *International Conference on Learning Representations (ICLR)*, (San Diego, CA, USA), 2015.
- [32] H. Hersbach, B. Bell, P. Berrisford, S. Hirahara, A. Horányi, J. Muñoz-Sabater, J. Nicolas, C. Peubey, R. Radu, D. Schepers, A. Simmons, C. Soci, S. Abdalla, X. Abellan, G. Balsamo, P. Bechtold, G. Biavati, J. Bidlot, M. Bonavita, G. De Chiara, P. Dahlgren, D. Dee, M. Diamantakis, R. Dragani, J. Flemming, R. Forbes, M. Fuentes, A. Geer, L. Haimberger, S. Healy, R. J. Hogan, E. Hólm, M. Janisková, S. Keeley, P. Laloyaux, P. Lopez, C. Lupu, G. Radnoti, P. de Rosnay, I. Rozum, F. Vamborg, S. Villaume, and J.-N. Thépaut, “The ERA5 global reanalysis,” *Quarterly Journal of the Royal Meteorological Society*, vol. 146, no. 730, pp. 1999–2049, 2020. eprint: <https://onlinelibrary.wiley.com/doi/pdf/10.1002/qj.3803>.
- [33] J. P. Dunne, L. W. Horowitz, A. J. Adcroft, P. Ginoux, I. M. Held, J. G. John, J. P. Krasting, S. Malyshev, V. Naik, F. Paulot, E. Shevliakova, C. A. Stock, N. Zadeh, V. Balaji, C. Blanton, K. A. Dunne, C. Dupuis, J. Durachta, R. Dussin, P. P. G. Gauthier, S. M. Griffies, H. Guo, R. W. Hallberg, M. Harrison, J. He, W. Hurlin, C. McHugh, R. Menzel, P. C. D. Milly, S. Nikonov,

- D. J. Paynter, J. Ploshay, A. Radhakrishnan, K. Rand, B. G. Reichl, T. Robinson, D. M. Schwarzkopf, L. T. Sentman, S. Underwood, H. Vahlenkamp, M. Winton, A. T. Wittenberg, B. Wyman, Y. Zeng, and M. Zhao, “The GFDL Earth System Model Version 4.1 (GFDL-ESM 4.1): Overall Coupled Model Description and Simulation Characteristics,” *Journal of Advances in Modeling Earth Systems*, vol. 12, no. 11, p. e2019MS002015, 2020. .eprint: <https://onlinelibrary.wiley.com/doi/pdf/10.1029/2019MS002015>.
- [34] A. J. Cannon, S. R. Sobie, and T. Q. Murdock, “Bias correction of gcm precipitation by quantile mapping: how well do methods preserve changes in quantiles and extremes?,” *Journal of Climate*, vol. 28, no. 17, pp. 6938–6959, 2015.

## Acknowledgments

### Funding

Funded under the Excellence Strategy of the Federal Government and the Länder through the TUM Innovation Network EarthCare.

This is ClimTip contribution #X; the ClimTip project has received funding from the European Union's Horizon Europe research and innovation programme under grant agreement No. 101137601.

PH, SB, and NB acknowledge funding by the Volkswagen Foundation.

YH acknowledges funding by the Alexander von Humboldt Foundation.

### Author contributions

#### Data Availability

The ERA5 reanalysis data is available for download at the Copernicus Climate Change Service (<https://cds.climate.copernicus.eu/cdsapp#!/dataset/reanalysis-era5-single-levels?tab=overview>). The CMIP6 GFDL-ESM4 is available at <https://esgf-data.dkrz.de/search/cmip6-dkrz/>. All data are available in the main text or the supplementary materials.

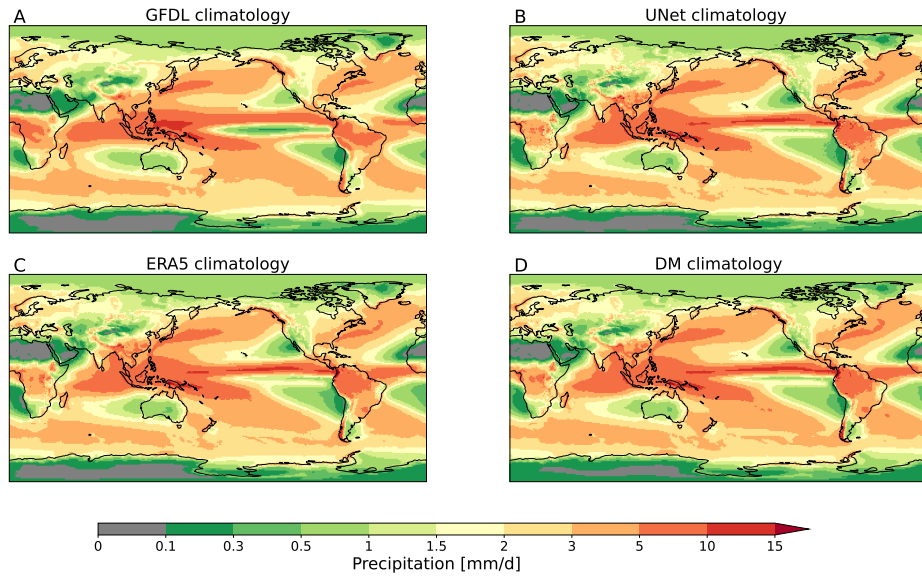
#### Code Availability

The code will be made available on GitHub and Zenodo.

#### Competing interests

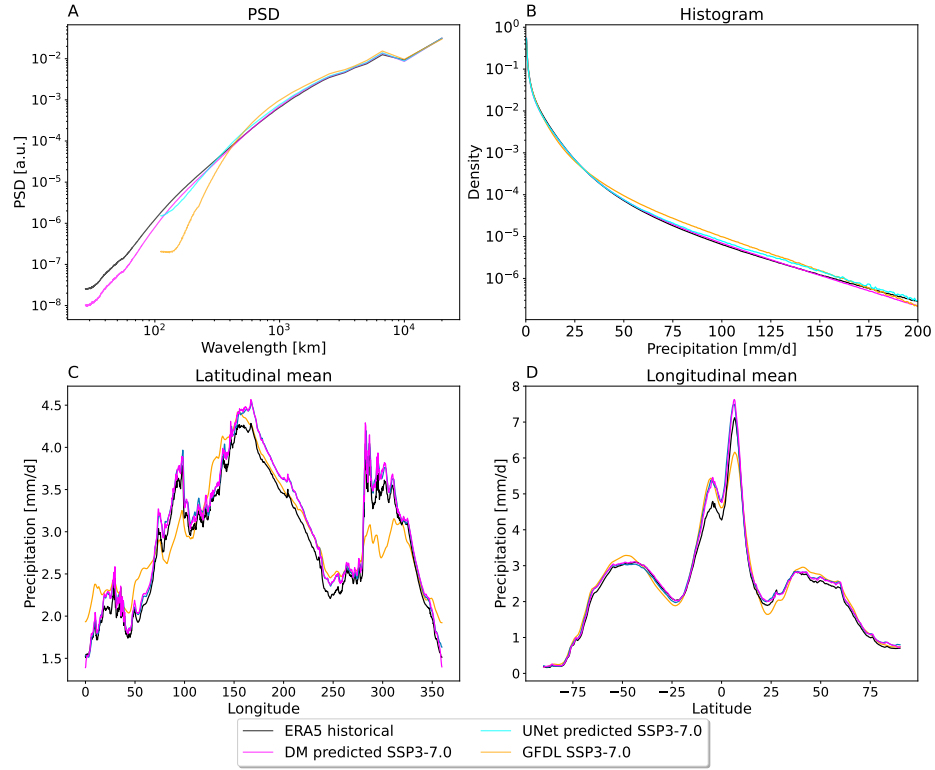
The authors declare no competing interests.

Fig. S1



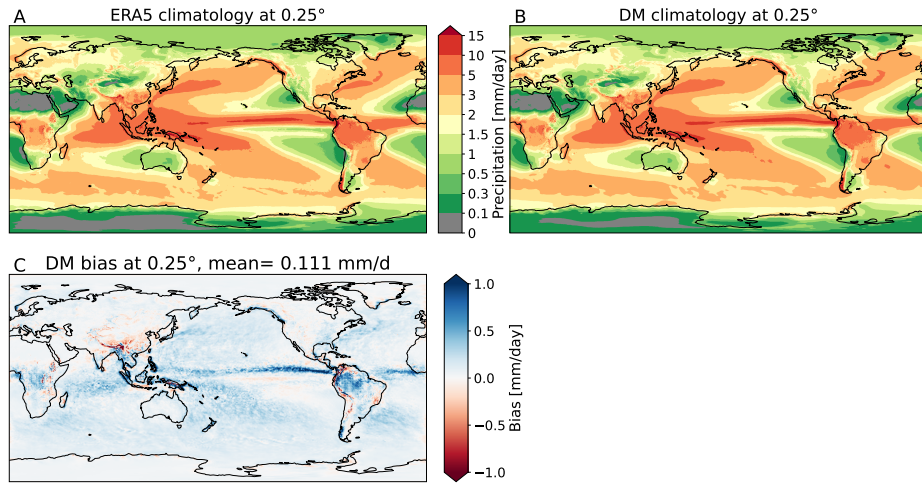
**Fig. S1 Comparing long term climatologies.** Both our regression model and our diffusion model show climatologies that are closely aligned with ERA5. In contrast, GFDL exhibits a notable ITCZ shift compared to our regression and diffusion models. Note that we downsampled ERA5 and the diffusion model to 1° using average pooling for comparability.

Fig. S2



**Fig. S2 Comparing the statistics of different models in the SSP3-7.0 scenario.** The mean spatial power spectral density (PSD) shows that our diffusion model (magenta) improves the small-scale spatial variability and is able to increase the resolution of our regression model (cyan) from  $1^\circ$  to  $0.25^\circ$  (A). There is a large agreement in the large spatial scales and only a slight disagreement compared to ERA5 (black) for the very small scales. GFDL (yellow) and our regression model (both at  $1^\circ$ ) have mismatches throughout the spectrum that get increasingly larger for smaller-scales in the case of GFDL. In the following comparisons, we bi-linearly upsampled the GFDL and our regression model's predicted precipitation (orange/cyan) from  $1^\circ$  to the  $0.25^\circ$  resolution of ERA5 and the diffusion model. The histogram (B) shows large improvements of our models compared to GFDL with slight deviations from the HR ERA5 reference data only for the extreme precipitation events. The regression model is always further away from ERA5 than the DM, except for the very extreme precipitation. The Latitude/Longitude (C)/(D) profiles are given by the averaged longitudes/latitudes show that our regression model and our diffusion model approximate the latitude and longitude profile of the original ERA5 reference data much better than GFDL. The longitude profile is weighted by the cosine of latitude to account for the varying grid cell area.

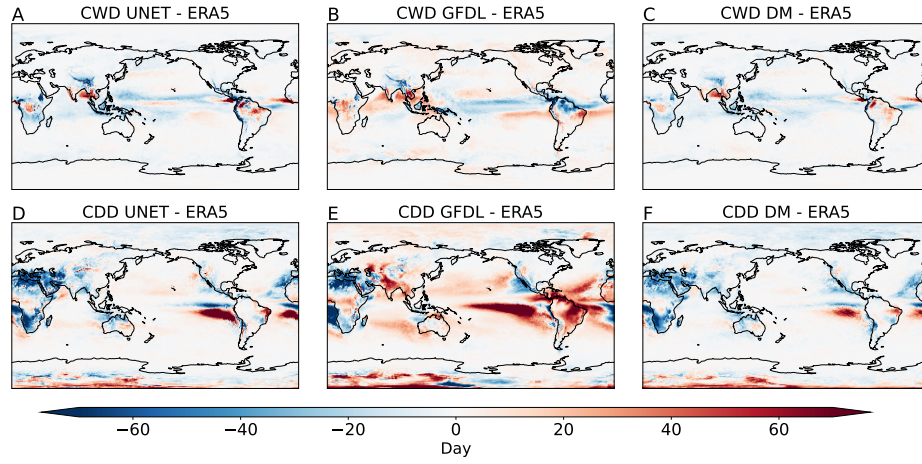
**Fig. S3**



**Fig. S3** Comparison of the long-term precipitation climatology of ERA5 and the precipitation predicted by our diffusion model at 0.25°. The climatologies align well, with no indication of a double ITCZ bias in our model. The difference map, along with a low mean absolute bias of 0.111 mm/d, highlights a very minimal bias in our diffusion model.

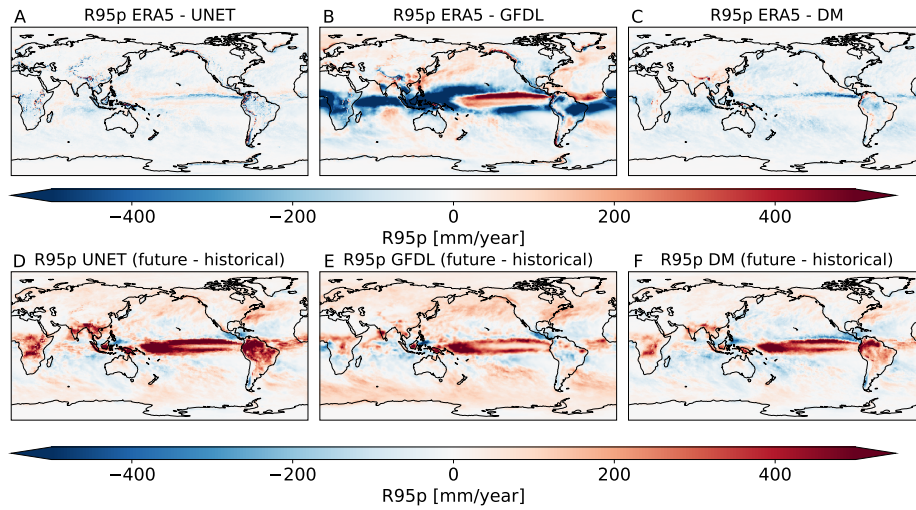


Fig. S4



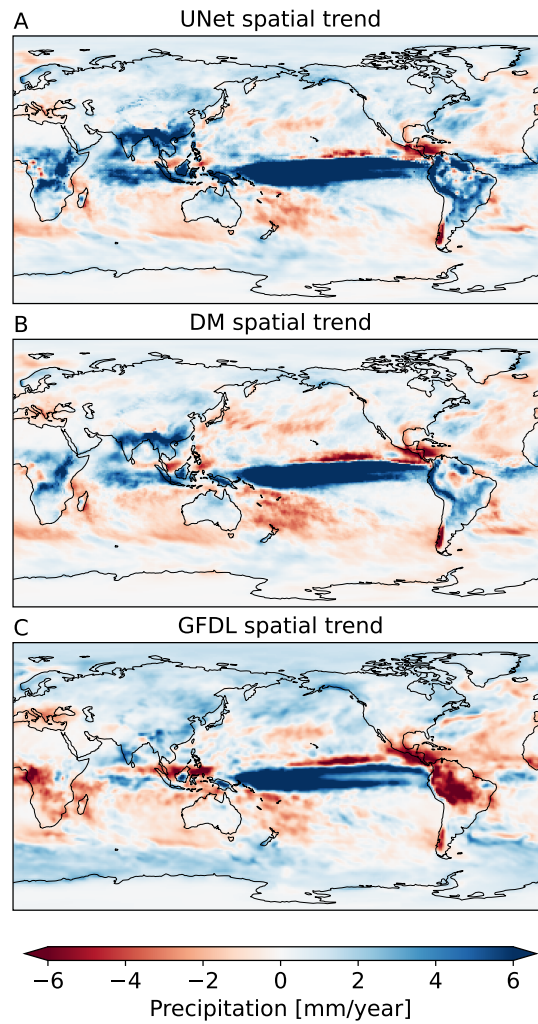
**Fig. S4 Comparing consecutive wet days (CWD) and consecutive dry days for the historical period 1980-2005.** We show the CWD-differences (top row) and CDD-differences (bottom row) compared to ERA5. Panels (A–C) show CWD anomalies from the regression model, GFDL, and the diffusion model, respectively, while panels (D–F) display CDD anomalies for the same three datasets. Red areas indicate an increase relative to ERA5, and blue areas a decrease. Our DM has overall the smallest bias compared to ERA5, especially improving the wet-bias around the tropics of GFDL

**Fig. S5**



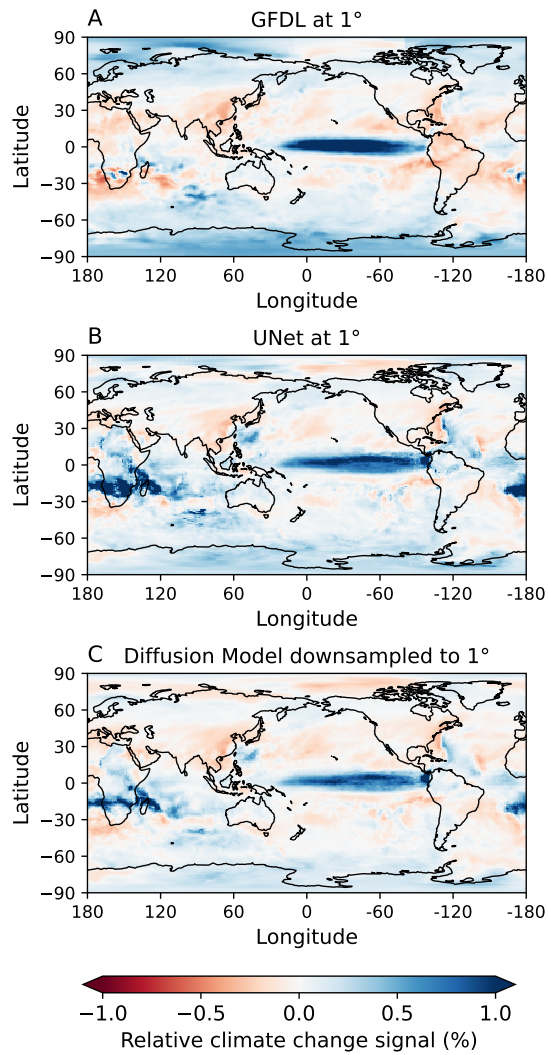
**Fig. S5 Evaluating extreme event coverage for historical and future scenarios.** We compare the total precipitation from days exceeding the 95th percentile of daily rainfall (R95p). **(A-C)**: Bias in historical data (1980 - 2005), showing R95p relative to ERA5. **(A)** UNet bias (ERA5 - UNet), **(B)** GFDL bias (ERA5 - GFDL), and **(C)** DM bias (ERA5 - DM). Negative values (blue) indicate overestimation of extreme precipitation by the respective model, while positive values (red) indicate underestimation. The GFDL model exhibits strong wet biases in the tropics during the historical period **(B)**, whereas the DM and UNet models show reduced biases **(A, C)**. Bottom row **(D-F)**: Projected changes in R95p between the late 21st century (2075 - 2100, SSP3-7.0) and the historical period. **(D)** UNet future change (future - historical), **(E)** GFDL future change, and **(F)** DM future change. Positive values (red) indicate an intensification of extreme precipitation, while negative values (blue) indicate reductions. Under future warming, all models predict an increase in R95p over the tropics. Overall, GFDL shows the strongest intensification of precipitation, while DM and UNet exhibit a more modest increase.

Fig. S6



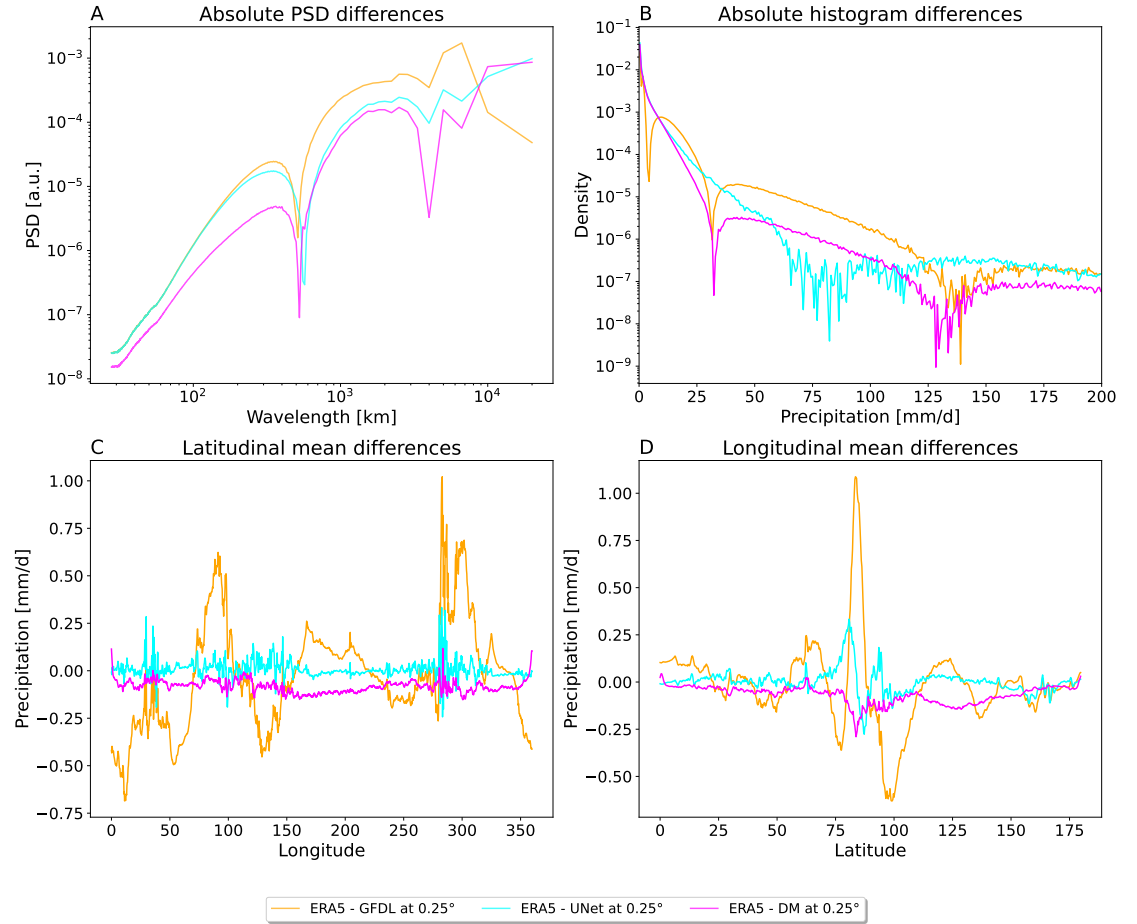
**Fig. S6** Our diffusion model (DM) preserves the spatial features of the trend from the UNet under the SSP3-7.0 scenario. (A-C) show the trend at each location between 2015 and 2100 for the UNet, DM, and GFDL as a reference. For comparison, we downsampled the DM precipitation fields to the  $1^\circ$  resolution of the UNet and GFDL. While the DM preserves the spatial trend patterns of the UNet, it adjusts the overall trend to be smaller.

Fig. S7



**Fig. S7 Relative precipitation changes (%)**. All changes compare the late 21st century (2075-2100) under the SSP3.7.0 scenario and the present-day period (1980-2005). **(A)** GFDL precipitation, **(B)** the UNet regression model, and **(C)** our diffusion model. The sign of the change is mostly consistent across the maps. The diffusion model predicts a slightly weaker change than the regression model but maintains similar spatial patterns.

**Fig. S8**



**Fig. S8 Visualizing the differences between models with respect to ERA5 statistics at 0.25° resolution over 40 years.** We compare the differences of GFDL (upsampled to 0.25°) in yellow, our UNet regression model (upsampled to 0.25°) in cyan, and our diffusion model (DM) at 0.25° in magenta. **(A)** Absolute difference in mean spatial power spectral density (PSD). The diffusion model has the overall smallest difference compared to ERA5. GFDL has much larger differences even in the large spatial scales. **(B)** Absolute differences in the histograms indicating differences in precipitation frequencies. The histogram also shows that our DM has the smallest deviation from ERA5 and is especially superior in the range of 10 mm/d - 60 mm/d. **(C)** Differences in the longitude profile, given by the data averaged over all longitudes, weighted by the cosine of latitude to account for the varying grid cell area. Both our DM and UNet model have much smaller deviations from ERA5 than GFDL. **(D)** Latitude profile, given by the data averaged over all longitudes. Our DM exhibits the smallest deviation from ERA5, while GFDL shows a pronounced ITCZ bias.